COVID-19 diagnosis in CT images using CNN to extract features and multiple classifiers

Edelson Damasceno Carvalho*, Edson Damasceno Carvalho‡, Antônio Oséas de Carvalho Filho †‡,
Alcilene Dalília de Sousa†§ and Ricardo de Andrade Lira Rabêlo ‡
*Information Systems, Federal University of Piauí, Simões, PI, Brazil
†Information Systems, Federal University of Piauí, Picos, PI, Brazil
‡Electrical Engineering, Federal University of Piauí, Teresina, PI, Brazil
§Teleinformatics Engineering, Federal University of Ceará, Fortaleza, CE, Brazil
edelsondamasceno@gmail.com, {edsondamasceno,antoniooseas,alcilene,ricardoalr}@ufpi.edu.br

***Abstract*—Coronavirus disease (COVID-19) has already infected more than 20 million people worldwide and is responsible for more than 744,000 deaths. A major problem faced in the diagnosis of COVID-19 is the inefficiency and scarcity of medical tests. The use of computed tomography (CT) has shown promise in the evaluation of patients with suspected COVID-19 infection. The analysis of the CT examination is complex and requires the effort of a specialist, which can lead to diagnostic errors. The use of CAD systems can minimize the problems generated by the analysis of CTs by specialists. This article presents a methodology for diagnosing COVID-19 using a trainable resource extractor using CNN and multiple classifiers. First, the quality of the images was improved using histogram equalization and CLAHE. Then, a basic CNN is used to extract resources from 708 CTs, 312 with COVID-19, and 396 Non-COVID-19. After the extracted data, we used multiple classifiers for classification in COVID-19 and Non-COVID-19. The results show an accuracy of 97.88%, recall of 97.77%, the precision of 97.94%, F-score of 0.978, AUC of 0.977, and kappa index of 0.957. The results obtained show that the proposed methodology can be used as a CAD system to aid in the diagnosis of COVID-19.**

***Index Terms*—COVID-19, diagnosis, histogram equalization, CLAHE, CNN feature extraction, CAD**

I. Introduction

Coronavirus disease 2019 (COVID-19) is a respiratory disease caused by infection with the severe acute respiratory syndrome 2 coronaviruses (SARS-CoV-2) [1]. COVID-19 has infected more than 20 million people worldwide and is responsible for more than 744,000 deaths [2]. Due to the unavailability of specific drugs for COVID-19, early diagnosis is essential for the cure and control of the disease [3].

The inefficiency and scarcity of medical examinations can lead infected people to be undiagnosed and not receive proper treatment [3]. Computed tomography (CT) can be used as an alternative tool to detect COVID-19, having high sensitivity, it is considered promising for the evaluation of patients with suspected COVID-19 infection [4], [5]. The main problem with this method is that it depends on the specialist to analyze the CT images, as the process is repetitive, time-consuming and tiring for the specialist, due to a large number of images to be analyzed, causing fatigue, which can lead to diagnostic errors [6]–[8].

To minimize the problems generated by image analysis by specialists, computer-aided diagnosis (CAD) systems appear as an alternative aid to medical diagnosis. These systems use computational power to analyze the images, being crucial for cases where the diagnosis is very difficult for the human eye [9], [10]. With technological advances, deep learning methods have been implemented in the development of CAD systems. Convolutional neural networks (CNN), which are deep learning techniques, can automatically interpret images [11]. However, the complexity of the model, difficulty in training, high computational cost, and the need for a large set of images, makes it difficult to develop a methodology using CNN with an effective application.

For the development of an efficient diagnostic model for COVID-19 using CNN, a large set of CT images is required. A strategy commonly used in the literature is the use of CNN as a resource extractor of medical images [12], [13]. The work shows that the resources extracted with CNN are generic and can be used for classification tasks outside the exact domain for which the networks were trained.

In this article, we propose a new scheme for diagnosing COVID-19. A trainable resource extractor using CNN is used to obtain more generic resources on CT images. Then, the extracted resources are used in multiple classifiers for classification in COVID-19 and Non-COVID-19. The experiments show that the proposed scheme presents promising results in the diagnosis of COVID-19. The rest of the paper is organized as follows. In Section II, we discuss related work. In Section III, we present the methodology used to extract features and classify the images. In Section IV, we present and discuss the results obtained. Finally, in Section V we present the conclusions and future work.

II. Related Works

The development of CAD systems to aid in medical diagnosis using CNN has shown to be very promising. CNN's can be implemented in CAD systems for resource extraction, classification or extraction, and classification. The efficiency of a CAD system is related to the techniques that compose it. In this sense, the literature shows studies using CNN for diagnosing COVID-19 in CT images. CNN's are easy to train

DOI 10.1109/BIBE50027.2020.00075

when there are large numbers of labeled samples that represent the different target classes. Due to the small number of images, it is not common to train a CNN with randomized weight initializations, as this would require a large number of images and a few weeks of training using multiple GPUs. Thus, a common practice is to use the weights of an already-trained network for a very large base, and then these weights can be used to initialize and retrain a network, or even to extract image characteristics [14], [15].

Since the emergence of COVID-19, there have been increasing efforts to develop deep learning methods for diagnosing COVID-19. Ozkaya et al. [16] proposed the use of pre-trained CNNs for diagnosing COVID-19 in a set of 150 CT images, presenting an accuracy of 98.27%, the sensitivity of 98.93%, a specificity of 97.60%, the precision of 97.63%, F-score of 0.982 and Matthews correlation coefficient (MCC) metrics of 96.54%. Wang et al. [17] proposed the use of the Inception network for diagnosing COVID-19 in a set of 1,065 CT images, reaching a total accuracy of 89.5%, with the specificity of 88% and sensitivity of 87%.

He et al. [18] proposed the use of learning transfer in a set of 746 CT images, reaching an F-score of 0.85 and an AUC of 0.94. Wang et al. [19] proposed the use of weak supervised CNN using 3D CT volumes for diagnosing COVID-19 in 630 CT volumes, obtaining an area under the ROC curve of 0.959 and area under the precision-recall curve of 0.976. Song et al. [20] proposed the use of a neural network of details ratio extraction (DRE-Net) to extract the resources of 777 CT images with COVID-19 and 1213 Non-COVID-19 images. Forecasts at the imaging level were aggregated to obtain diagnosis at the patient level. The model consists of using the pre-trained ResNet-50 network with the resource pyramid network to diagnose each image. The methodology presented an AUC of 0.99 and a recall of 93%.

As can be seen, solving the problem of classifying CT in COVID-19 and Non-COVID-19 is not a simple task. The use of CNN for resource extraction and classification requires a large number of images and parameter training to create efficient COVID-19 diagnostic models. The use of small sets of images can lead to over-adjustment of the model, performing well on the training data, but generalizing the test data poorly. Thus, we propose an approach for diagnosing COVID-19 in CT images using CNN for resource extraction and multiple classifiers.

III. Methodology

The proposed methodology consists of the classification of CT images in COVID-19 and Non-COVID-19. The proposed method is shown in Figure 1. The methodology consists of: i) CT image acquisition; ii) pre-processing using histogram equalization and CLAHE; iii) feature extraction using CNN; iv) classification of images using multiple classifiers and v) validation of results using metrics commonly used in the literature.

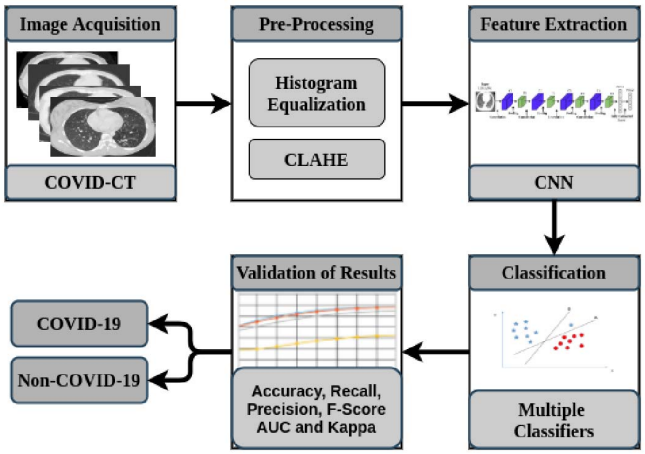

Fig. 1. Proposed methodology.

A. Image Acquisition

COVID-CT is a set of CT images developed by Zhao et al. [21] for binary classification of COVID-19. The set consists of 708 CTs, of which 312 COVID-19 and 396 Non-COVID-19. Figure 2 shows an example of images from COVID-CT, where, in (a) we have an example of CT COVID-19 and in (b) we have an example of CT Non-COVID-19.

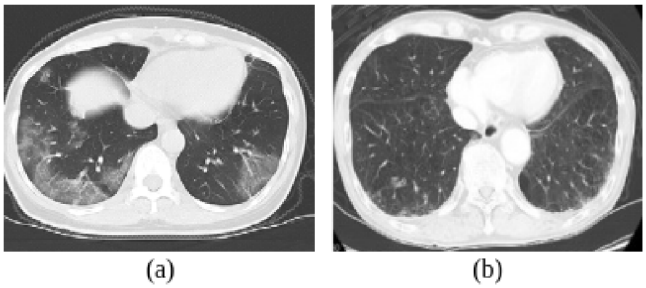

Fig. 2. Example images from COVID-CT, (a) CT COVID-19 and (b) CT Non-COVID-19.

COVID-CT images were collected from articles related to COVID-19 from medRxiv, bioRxiv, NEJM, JAMA, Lancet, etc. CTs containing abnormalities were selected by reading the captions of the figures in the documents. Non-COVID-19 images were collected from MedPix, LUNA, Radiopaedia website, and PubMed Central.

B. Pre-processing

Image pre-processing aims to improve image quality. COVID-CT is a set of images collected from articles, which may have a loss of quality. In this sense, histogram equalization and CLAHE were used to improve the quality of COVID-CT images.

- Histogram equalization (HE) is a method for improving the overall contrast of an image [22]. Given a grayscale image x and the number of gray level occurrences n_i,

the probability of occurrence of a pixel i in the image x is given by Equation 1.

$$p_x(i) = p(x = i) = \frac{n_i}{n}, 0 \leq i < L \quad (1)$$

Where, L is the total number of gray levels, n the total number of pixels and $p_x(i)$ the histogram of the image to the pixel value i, normalized to 0 or 1. Figure 3(b) presents an image of COVID-CT with the equalized histogram.

- O contrast limited adaptive histogram equalization (CLAHE) is a method that improves the local contrast of an image [23], [24]. CLAHE performs the histogram equalization of non-overlapping sub-areas of the image, correcting inconsistencies through interpolation. In this method, an enhancement function is applied over all neighboring pixels and the transformation function is derived [25]. Figure 3(c) shows an image of COVID-CT applied to CLAHE.

C. Feature extraction

In the development of an automatic image classification system, extracting quality resources is essential to obtain a more robust system [26]. The quality of the extracted resources can influence the classification performance, leading to a loss of performance by the system. In recent years, CNN models have been proposed for the resource extraction stage. CNN's have a hierarchical structure for learning resources with high quality in their layers.

A CNN consists of alternating layers of convolution and pooling, then turns into fully connected layers as it approaches the outgoing layer. Each of the CNN layers has a specific function in the propagation of the input signal. In this article, a basic CNN was used for the feature extraction step. CNN consists of: an input layer (Input), four convolution layers (C1, C2, C3, and C4), four pooling layers (P1, P2, P3, and P4) and two fully connected layers (FCL1 and FCL2). CNN's structure for resource extraction is shown in Figure 4. The Table I presents a summary of the CNN layers.

In a CNN, the convolutional layers are responsible for extracting attributes from the input volumes. The pooling layers are responsible for reducing the dimensionality of the resulting volume after the convolutional layers and help to make the representation invariant to small translations at the entrance. The fully connected layers are responsible for the propagation of the signal through point-to-point multiplication and the use of an activation function.

To use CNN as a feature extractor, we removed the last fully connected layer from the network (the layer that computes the probability of the input image belonging to one of the predetermined classes) and the final output (FCL2) was used as features that describe the input image. The characteristics extracted from the images were used in multiple classifiers that require less data for training. This feature extraction strategy is widely used for medical imaging applications [12], [27], of materials [28], [29], Content Based Image Retrieval - CBIR [30]–[32].

D. Classification

The classification process can be carried out considering the previously defined classes. The classification consists of recognizing which of a set of categories a new observation belongs, based on previous training on a data set that has observations whose category is known [33]. For the development of this work, the classification was made using the XGBoost, random forest, and multilayer perceptron classifiers.

- eXtreme Gradient Boosting (XGBoost) is a scalable and effective machine learning system for tree growth, proposed by Chen e Guestrin [34]. Tree augmentation is a learning algorithm that makes weak classifiers strong in classifying a data set. XGBoost is a tree method that applies the principle of driving weak learning using the descending gradient architecture. However, XGBoost improves the basic structure of Gradient Boosting Machines through system optimization and algorithmic improvements [34]. XGBoost can classify problems using a minimal amount of resources. The parameters used in XGBoost were as follows: max depth = 7, learning rate = 0.1, ite = 1000, gama = 0, max delta step = 1, and objective = "multi:softmax".
- Random forest (RF) is the random combination of multiple decision trees, combined to obtain a more stable and more accurate prediction [35]. The RF divides each node using the best of a subset of indicators chosen at random in that node. This strategy, although somewhat contradictory, works adequately in comparison with many other classifiers, in addition to being robust to overfitting parameters. Also, it is easy to use, as it has only two parameters: the number of variables in the random subset at each node and the number of trees in the forest. The parameters used were: bag size percent = 100, batch size = 100, number of execution slots = 1, max depth = 0 (unlimited), number of randomly chosen attributes = 0, number of iterations to be performed = 100, minimum number of instances per leaf = 1.0, minimum variance for split = 0.001, and random number seed to be used = 1.
- Multilayer perceptron (MLP) is a neural network with several layers of neurons connected through weighted synapses, which learns from the retro-propagation of the output error and updating the weights [36]. An MLP consists of at least three layers of nodes: an input layer, a hidden layer, and an output layer. Except for the input nodes, each node is a neuron that uses a nonlinear activation function. MLP uses backpropagation as a learning technique during training. Multiple layers and nonlinear activation distinguish MLP from a linear perceptron, managing to classify data that is not linearly separable. The parameters used in MLP were: learning rate = 0.3, momentum = 0.2, the number of epochs to train through = 500, validation set size = 0 (the network

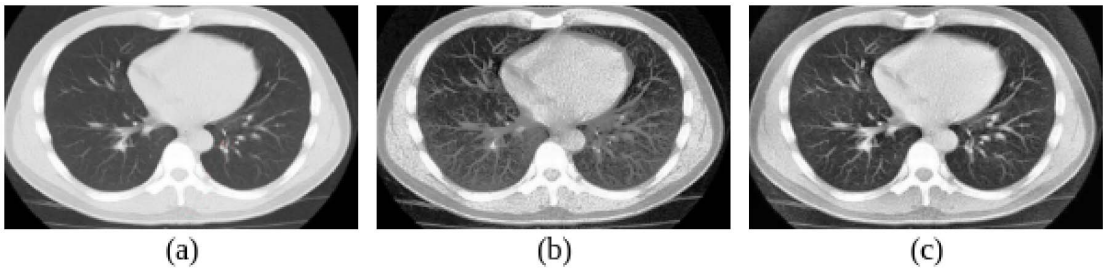

Fig. 3. Example of the pre-processed image, (a) original, (b) equalized histogram, and (c) CLAHE.

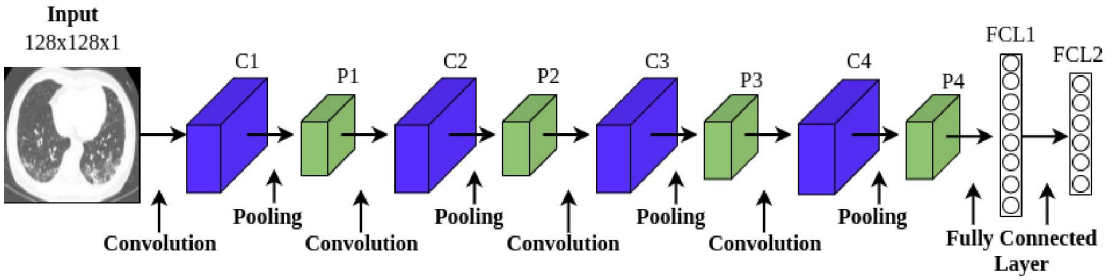

Fig. 4. CNN structure for resource extraction.

TABLE I
SUMMARY OF CNN LAYERS

Layer	No. of Kernels	Kernel size	Activation
Input	1	128 × 128	-
Convolution (C1)	32	5 × 5	ReLu
Pooling (P1)	-	3 × 3	-
Convolution (C2)	32	5 × 5	ReLu
Pooling (P2)	-	3 × 3	-
Convolution (C3)	32	5 × 5	ReLu
Pooling (P3)	-	3 × 3	-
Convolution (C4)	32	5 × 5	ReLu
Pooling (P4)	-	3 × 3	-
Fully connected (FCL1)	128	1 × 1	ReLu
Fully connected (FCL2)	100	1 × 1	ReLu

will train for the specified number of epochs), seed = 0, validation threshold = 20, and hidden layers = (number of attributes + classes)/2.

E. Validation of results

To validate the model, statistical evaluation metrics commonly used in the literature were used. These metrics are calculated based on the confusion matrix, given the number of true positives (TP), false positives (FP), true negatives (TN) and false negatives (FN), the measures are mathematically expressed as follows:

$$Accuracy = \frac{TP + TN}{TP + TN + FP + FN} \tag{2}$$

$$Precision = \frac{TP}{TP + FP} \tag{3}$$

$$Recall = \frac{TP}{TP + FN} \tag{4}$$

$$F - Score = 2 \times \frac{Recall \times Precision}{Recall + Precision} \tag{5}$$

The Area under ROC curve (AUC) it is a performance measure for the classification problem in various threshold configurations. AUC is a measure of separability. The higher the AUC, the better the model can distinguish between classes. By analogy, the higher the AUC, the better the model can distinguish between patients with and without disease.

The Kappa index (K) measures the agreement between the results presented by the developed methodology and the truth of the human terrain labeled by pathologists [37]. The Kappa index interpretation scale is shown in Table II. The closer the Kappa value is to 1, the greater the agreement.

IV. RESULT AND DISCUSSION

In this section, we present the results obtained in the proposed methodology to classify CT images in COVID-19 and Non-COVID-19. To extract resources from the CNN

TABLE II
LEVELS OF CLASSIFICATION ACCURACY ACCORDING TO THE KAPPA INDEX.

Índice Kappa (k)	Quality
$K < 0.2$	Poor
$0.2 \leq K < 0.4$	Reasonable
$0.4 \leq K < 0.6$	Good
$0.6 \leq K < 0.8$	Very good
$K \geq 0.8$	Excellent

model, we need to train the network. CNN training is carried out so that it can extract more robust resources from the image. After training CNN 200 times, a set of 100 resources was extracted from each image. After extracting the characteristics of the 708 CT images, the classification was made using multiple classifiers with cross-validation of k-folds, with k = 5. Table III shows the results obtained.

As can be seen in the table III, using the original images, the characteristics extracted using CNN together with XGBoost obtained the best results. Applying the histogram equalization, the random forest obtained the best results. Applying CLAHE, XGBoost achieved the best results. It can be seen that the use of pre-processing helped CNN to obtain characteristics that better discriminate between CT images in COVID-19 and Non-COVID-19. The methodology using CLAHE, CNN, and XGBoost obtained the best results, with an accuracy of 97.88%, recall of 97.77%, the precision of 97.94%, F-score of 0.978, AUC of 0.977 and kappa of 0.957. The kappa index presented by the proposed methodology according to Table II shows that the classifiers obtained excellent results in the categorization of COVID-19. The use of CLAHE improved the quality of the images, making CNN obtain these more robust features to diagnose COVID-19 in CT images. The resources extracted with CNN are quite robust for categorizing images in COVID-19 and Non-COVID-19. Thus, the proposed methodology presented promising results, which can be used as a CAD system, assisting the specialist with a second opinion in the diagnosis of COVID-19.

In Table IV we compare the results obtained with the proposed methodology with those presented in the related works. The comparison of results is very complex, as many factors can influence a reliable comparison. Thus, a summary of the results obtained with the proposed methodology and those presented in the related works are presented.

As can be seen in Table IV, the proposed methodology presents promising results in the classification of CT images in COVID-19 and Non-COVID-19, compared to those presented in related works. The methodology proposed by Ozkaya et al. [16] obtained slightly better results than those presented in the proposed methodology, except for precision. The proposed methodology presented better results than using the Inception network [17], learning transfer [18], and CNN supervised by weak [19]. Song et al. [20] obtained an AUC of 0.99 and a recall of 93%, while the proposed methodology obtained an AUC of 0.977 and a recall of 97.77%. Taking into account that the recall is the correctness rate of cases with COVID-19, the proposed methodology presented better results than those presented by Song et al. [20]. The use of different approaches makes the efficient comparison of the results of the proposed methodology with the related works very complex.

V. CONCLUSION

In this work, we present a methodology for diagnosing COVID-19 on CT images. Initially, pre-processing was applied to the images using the histogram equalization and CLAHE, then extracted a set of 100 resources from each image using a basic CNN, with the set of resources extracted, performed the classification using multiple classifiers. The use of pre-processing helped to improve the quality of the images. The resources extracted with the CNN architecture used were quite robust, obtaining an accuracy of 97.88%, recall of 97.77%, the precision of 97.94%, F-score of 0.978, AUC of 0.977 and kappa index of 0.957. Thus, the proposed methodology can be used by a specialist in the diagnosis of COVID-19, providing a second opinion in the diagnosis of the patient.

The proposed methodology can still be improved, as future works, we intended to use other sets of images from COVID-19, for the development of a complete methodology using CNN. Also, use other CNN architectures to extract resources from CT images, such as ResNet-50, VGG16, and VGG19. Thus, it is intended to obtain a more robust methodology in the diagnosis of COVID-19, which can assist the specialist in the final diagnosis

ACKNOWLEDGMENT

The proposed method was supported by the following institutions: FAPEPI - www.fapepi.pi.gov.br (5492.UNI253.59248.15052018); CAPES - www.capes.gov.br; and the CNPq - www.cnpq.br (435244/2018-3).

REFERENCES

[1] A. E. Gorbalenya, S. C. Baker, R. S. Baric, R. J. de Groot, C. Drosten, A. A. Gulyaeva, B. L. Haagmans, C. Lauber, A. M. Leontovich, B. W. Neuman, D. Penzar, S. Perlman, L. L. Poon, D. Samborskiy, I. A. Sidorov, I. Sola, and J. Ziebuhr, "Severe acute respiratory syndrome-related coronavirus: The species and its viruses – a statement of the coronavirus study group," *bioRxiv*, 2020. [Online]. Available: https://www.biorxiv.org/content/early/2020/02/11/2020.02.07.937862

[2] W. H. O. WHO. (2020, June) Coronavirus disease (covid-19) outbreak situation. [Online]. Available: https://www.who.int/emergencies/diseases/novel-coronavirus-2019

[3] D. Singh, V. Kumar, Vaishali, and M. Kaur, "Classification of covid-19 patients from chest ct images using multi-objective differential evolution-based convolutional neural networks," *European journal of clinical microbiology infectious diseases : official publication of the European Society of Clinical Microbiology*, April 2020. [Online]. Available: https://europepmc.org/articles/PMC7183816

[4] A. Bernheim, X. Mei, M. Huang, Y. Yang, Z. A. Fayad, N. Zhang, K. Diao, B. Lin, X. Zhu, K. Li, S. Li, H. Shan, A. Jacobi, and M. Chung, "Chest ct findings in coronavirus disease-19 (covid-19): Relationship to duration of infection," *Radiology*, vol. 0, no. 0, p. 200463, 2020, pMID: 32077789. [Online]. Available: https://doi.org/10.1148/radiol.2020200463

[5] D. Wang, B. Hu, C. Hu, F. Zhu, X. Liu, J. Zhang, B. Wang, H. Xiang, Z. Cheng, Y. Xiong, Y. Zhao, Y. Li, X. Wang, and Z. Peng, "Clinical Characteristics of 138 Hospitalized Patients With 2019 Novel Coronavirus–Infected Pneumonia in Wuhan, China," *JAMA*, vol. 323, no. 11, pp. 1061–1069, 03 2020. [Online]. Available: https://doi.org/10.1001/jama.2020.1585

TABLE III
RESULTS OF THE PROPOSED METHODOLOGY

Experiment	Classifier	Accuracy (%)	Recall (%)	Precision (%)	F-Score	AUC	Kappa
Original Image	XGBoost	**93.66**	**92.65**	**93.73**	**0.931**	**0.926**	**0.862**
	Random Forest	92.95	92.38	93.53	0.927	0.923	0.855
	MLP	92.25	92.07	92.21	0.921	0.920	0.842
Histogram equalization	XGBoost	94.36	94.58	94.48	0.943	0.945	0.887
	Random Forest	**95.85**	**95.88**	**95.62**	**0.957**	**0.958**	**0.914**
	MLP	92.95	93.34	92.83	0.929	0.933	0.858
CLAHE	XGBoost	**97.88**	**97.77**	**97.94**	**0.978**	**0.977**	**0.957**
	Random Forest	97.18	97.10	97.40	0.971	0.971	0.943
	MLP	94.36	94.28	94.56	0.943	0.942	0.887

TABLE IV
COMPARISON OF THE RESULTS OF THE PROPOSED METHODOLOGY WITH THE RELATED WORKS

Works	Accuracy	Recall	Precision	F-score	AUC
[16]	98.27%	98,93%	97.63%	0.982	-
[17]	89.5%	87%	-	-	-
[18]	-	-	-	0.85	0.94
[19]	-	-	-		0.959
[20]	-	93%	-	-	0.99
Our work	**97.88%**	**97.77%**	**97.94%**	**0.978**	**0.977**

[6] W. de Oliveira Torres, A. O. de Carvalho Filho, R. de Andrade Lira Rabêlo, and R. R. V. e Silva], "Texture analysis of lung nodules in computerized tomography images using functional diversity," *Computers Electrical Engineering*, vol. 84, p. 106618, 2020. [Online]. Available: http://www.sciencedirect.com/science/article/pii/S0045790620304730

[7] X. Liu, F. Hou, H. Qin, and A. Hao, "Multi-view multi-scale cnns for lung nodule type classification from ct images," *Pattern Recognition*, vol. 77, pp. 262 – 275, 2018. [Online]. Available: http://www.sciencedirect.com/science/article/pii/S0031320317305186

[8] A. O. de Carvalho Filho, A. C. Silva, A. C. de Paiva, R. A. Nunes, and M. Gattass, "Classification of patterns of benignity and malignancy based on ct using topology-based phylogenetic diversity index and convolutional neural network," *Pattern Recognition*, vol. 81, pp. 200 – 212, 2018. [Online]. Available: http://www.sciencedirect.com/science/article/pii/S0031320318301237

[9] E. D. Carvalho, A. O. [de Carvalho Filho], A. D. [de Sousa], A. C. Silva, and M. Gattass, "Method of differentiation of benign and malignant masses in digital mammograms using texture analysis based on phylogenetic diversity," *Computers Electrical Engineering*, vol. 67, pp. 210 – 222, 2018. [Online]. Available: http://www.sciencedirect.com/science/article/pii/S0045790617334663

[10] A. S. V. de Carvalho Junior, E. D. Carvalho, A. O. de Carvalho Filho, A. D. de Sousa, A. C. Silva], and M. Gattass, "Automatic methods for diagnosis of glaucoma using texture descriptors based on phylogenetic diversity," *Computers Electrical Engineering*, vol. 71, pp. 102 – 114, 2018. [Online]. Available: http://www.sciencedirect.com/science/article/pii/S0045790617338570

[11] O. Gozes, M. Frid-Adar, H. Greenspan, P. D. Browning, H. Zhang, W. Ji, A. Bernheim, and E. Siegel, "Rapid ai development cycle for the coronavirus (covid-19) pandemic: Initial results for automated detection patient monitoring using deep learning ct image analysis," 2020.

[12] R. Zhu, R. Zhang, and D. Xue, "Lesion detection of endoscopy images based on convolutional neural network features," in *2015 8th International Congress on Image and Signal Processing (CISP)*, 2015, pp. 372–376.

[13] B. van Ginneken, A. A. A. Setio, C. Jacobs, and F. Ciompi, "Off-the-shelf convolutional neural network features for pulmonary nodule detection in computed tomography scans," in *2015 IEEE 12th International Symposium on Biomedical Imaging (ISBI)*, 2015, pp. 286–289.

[14] Z. Zhou, J. Shin, L. Zhang, S. Gurudu, M. Gotway, and J. Liang, "Fine-tuning convolutional neural networks for biomedical image analysis: Actively and incrementally," in *The IEEE Conference on Computer Vision and Pattern Recognition (CVPR)*, July 2017.

[15] N. Bayramoglu and J. Heikkilä, "Transfer learning for cell nuclei classification in histopathology images," in *Computer Vision – ECCV 2016 Workshops*, G. Hua and H. Jégou, Eds. Cham: Springer International Publishing, 2016, pp. 532–539.

[16] U. Ozkaya, S. Ozturk, and M. Barstugan, "Coronavirus (covid-19) classification using deep features fusion and ranking technique," *arXiv preprint arXiv:2004.03698*, 2020.

[17] X. Wang, X. Deng, Q. Fu, Q. Zhou, J. Feng, H. Ma, W. Liu, and C. Zheng, "A weakly-supervised framework for covid-19 classification and lesion localization from chest ct," *IEEE Transactions on Medical Imaging*, pp. 1–1, 2020.

[18] X. He, X. Yang, S. Zhang, J. Zhao, Y. Zhang, E. Xing, and P. Xie, "Sample-efficient deep learning for covid-19 diagnosis based on ct scans," *medRxiv*, 2020. [Online]. Available: https://www.medrxiv.org/content/early/2020/04/17/2020.04.13.20063941

[19] S. Wang, B. Kang, J. Ma, X. Zeng, M. Xiao, J. Guo, M. Cai, J. Yang, Y. Li, X. Meng, and B. Xu, "A deep learning algorithm using ct images to screen for corona virus disease (covid-19)," *medRxiv*, 2020. [Online]. Available: https://www.medrxiv.org/content/early/2020/04/24/2020.02.14.20023028

[20] Y. Song, S. Zheng, L. Li, X. Zhang, X. Zhang, Z. Huang, J. Chen, H. Zhao, Y. Jie, R. Wang, Y. Chong, J. Shen, Y. Zha, and Y. Yang, "Deep learning enables accurate diagnosis of novel coronavirus (covid-19) with ct images," *medRxiv*, 2020. [Online]. Available: https://www.medrxiv.org/content/early/2020/02/25/2020.02.23.20026930

[21] J. Zhao, X. He, X. Yang, Y. Zhang, S. Zhang, and P. Xie, "Covid-ct-dataset: A ct scan dataset about covid-19," 2020.

[22] G. Yadav, S. Maheshwari, and A. Agarwal, "Contrast limited adaptive histogram equalization based enhancement for real time video system," in *2014 International Conference on Advances in Computing, Communications and Informatics (ICACCI)*, 2014, pp. 2392–2397.

[23] S. M. Pizer, E. P. Amburn, J. D. Austin, R. Cromartie, A. Geselowitz, T. Greer, B. T. H. Romeny, and J. B. Zimmerman, "Adaptive histogram equalization and its variations," *Comput. Vision Graph. Image Process.*, vol. 39, no. 3, p. 355–368, Sep. 1987. [Online]. Available: https://doi.org/10.1016/S0734-189X(87)80186-X

[24] K. Zuiderveld, *Contrast Limited Adaptive Histogram Equalization*. USA: Academic Press Professional, Inc., 1994, p. 474–485.

[25] G. Park, H. Cho, and M. Choi, "A contrast enhancement method using dynamic range separate histogram equalization," *IEEE Transactions on Consumer Electronics*, vol. 54, no. 4, pp. 1981–1987, 2008.

[26] X. Ren, H. Guo, S. Li, S. Wang, and J. Li, "A novel image classification method with cnn-xgboost model," 07 2017, pp. 378–390.

[27] B. van Ginneken, A. A. A. Setio, C. Jacobs, and F. Ciompi, "Off-the-shelf convolutional neural network features for pulmonary nodule detection in computed tomography scans," in *2015 IEEE 12th International Symposium on Biomedical Imaging (ISBI)*, 2015, pp. 286–289.

[28] S. Bell, P. Upchurch, N. Snavely, and K. Bala, "Material recognition in the wild with the materials in context database," *2015 IEEE Conference on Computer Vision and Pattern Recognition (CVPR)*, Jun 2015. [Online]. Available: http://dx.doi.org/10.1109/CVPR.2015.7298970

[29] Yan Zhang, M. Ozay, Xing Liu, and T. Okatani, "Integrating deep features for material recognition," in *2016 23rd International Conference on Pattern Recognition (ICPR)*, 2016, pp. 3697–3702.

[30] X. Liu, H. Tizhoosh, and J. Kofman, "Generating binary tags for fast medical image retrieval based on convolutional nets and radon transform," *2016 International Joint Conference on Neural Networks (IJCNN)*, Jul 2016. [Online]. Available: http://dx.doi.org/10.1109/IJCNN.2016.7727562

[31] L. Wang and X. Wang, "Model and metric choice of image retrieval system based on deep learning," in *2016 9th International Congress on Image and Signal Processing, BioMedical Engineering and Informatics (CISP-BMEI)*, 2016, pp. 390–395.
[32] R. Fu, B. Li, Y. Gao, and W. Ping, "Content-based image retrieval based on cnn and svm," 10 2016, pp. 638–642.
[33] B. D. Ripley, *Pattern Recognition and Neural Networks*. Cambridge University Press, 1996.
[34] T. Chen and C. Guestrin, "Xgboost: A scalable tree boosting system," in *Proceedings of the 22nd ACM SIGKDD International Conference on Knowledge Discovery and Data Mining*, ser. KDD '16. New York, NY, USA: Association for Computing Machinery, 2016, p. 785–794. [Online]. Available: https://doi.org/10.1145/2939672.2939785
[35] L. Breiman, "Random forests," *Machine Learning*, vol. 45, no. 1, pp. 5–32, Oct 2001.
[36] S. Russell and P. Norvig, *Artificial Intelligence: A Modern Approach*, 3rd ed. Upper Saddle River, NJ, USA: Prentice Hall Press, 2009.
[37] J. R. Landis and G. G. Koch, "The measurement of observer agreement for categorical data," *Biometrics*, vol. 33, no. 1, pp. 159–174, 1977. [Online]. Available: http://www.jstor.org/stable/2529310